

# Regulation of activity and localization of the WNK1 protein kinase by hyperosmotic stress

Anna Zagórska,<sup>1</sup> Eulalia Pozo-Guisado,<sup>1</sup> Jérôme Boudeau,<sup>1</sup> Alberto C. Vitari,<sup>1</sup> Fatema H. Rafiqi,<sup>1</sup> Jacob Thastrup,<sup>1</sup> Maria Deak,<sup>1</sup> David G. Campbell,<sup>1</sup> Nick A. Morrice,<sup>1</sup> Alan R. Prescott,<sup>2</sup> and Dario R. Alessi<sup>1</sup>

<sup>1</sup>Medical Research Council Protein Phosphorylation Unit and <sup>2</sup>Division of Cell Biology and Immunology, School of Life Sciences, Medical Sciences Institute/Wellcome Trust Biocentre Complex, University of Dundee, Dundee DD1 5EH, Scotland, UK

**M**utations within the WNK1 (with-no-K[Lys] kinase-1) gene cause Gordon's hypertension syndrome. Little is known about how WNK1 is regulated. We demonstrate that WNK1 is rapidly activated and phosphorylated at multiple residues after exposure of cells to hyperosmotic conditions and that activation is mediated by the phosphorylation of its T-loop Ser382 residue, possibly triggered by a transautophosphorylation reaction. Activation of WNK1 coincides with the phosphorylation and activation of two WNK1 substrates, namely, the protein kinases STE20/SPS1-related proline alanine-rich kinase (SPAK) and oxidative stress response kinase-1 (OSR1). Small interfering RNA depletion of

WNK1 impairs SPAK/OSR1 activity and phosphorylation of residues targeted by WNK1. Hyperosmotic stress induces rapid redistribution of WNK1 from the cytosol to vesicular structures that may comprise trans-Golgi network (TGN)/recycling endosomes, as they display rapid movement, colocalize with clathrin, adaptor protein complex 1 (AP-1), and TGN46, but not the AP-2 plasma membrane-coated pit marker nor the endosomal markers EEA1, Hrs, and LAMP1. Mutational analysis suggests that the WNK1 C-terminal noncatalytic domain mediates vesicle localization. Our observations shed light on the mechanism by which WNK1 is regulated by hyperosmotic stress.

## Introduction

WNK1 (with-no-K[Lys] kinase-1) was originally identified as an unusual kinase that lacked an invariant catalytic Lys residue in subdomain II of the catalytic domain that is crucial for binding of ATP (Xu et al., 2000). WNK1 is a catalytically active kinase, and modeling (Xu et al., 2000), as well as structural analysis, of the WNK1 catalytic domain (Min et al., 2004) revealed that a Lys residue in subdomain I substitutes for the missing Lys residue in subdomain II. WNK1 is a widely expressed protein kinase comprising 2,382 residues. It possesses a kinase catalytic domain at its N terminus (residues 221–479), and apart from three putative coiled-coil domains, the remainder of the WNK1 polypeptides possess no obvious structural features (Verissimo and Jordan, 2001; Xu et al., 2005). Great interest in WNK1 was aroused after the finding that intronic

deletions that increased WNK1 expression were observed in humans with an inherited hypertension and hyperkalemia (elevated plasma K<sup>+</sup>) disorder termed Gordon's syndrome or pseudohypaldosteronism type II (OMIM 145260; Wilson et al., 2001). These findings indicated that overexpression of WNK1 may result in hypertension and, consistent with this, heterozygous WNK1<sup>-/+</sup> mice possess reduced blood pressure (Zambrowicz et al., 2003). WNK1-knockout embryos fail to develop, indicating that WNK1 is also required for normal development. There are four isoforms of WNK (WNK1, -2, -3, and -4) in humans encoded by distinct genes (Verissimo and Jordan, 2001). Mutations in WNK4 have also been found in patients with Gordon's syndrome, but in contrast to WNK1, these comprise point mutations lying within noncatalytic regions of this enzyme (Wilson et al., 2001). It is not yet clear how mutations in WNK4 lead to Gordon's syndrome, but overexpression of a Gordon's syndrome mutant of WNK4, but not the wild-type enzyme, increased blood pressure in mice (Lalioi et al., 2006).

Most functional studies on WNK isoforms have focused on the overexpression of these enzymes in *Xenopus laevis* oocytes or epithelial cells and monitoring the effects that this has on the activity and membrane localization of

A. Zagórska, E. Pozo-Guisado, J. Boudeau, A.C. Vitari, and F.H. Rafiqi contributed equally to this paper.

Correspondence to Dario R. Alessi: d.r.alessi@dundee.ac.uk

Abbreviations used in this paper: CCT, conserved C-terminal; ERK, extracellular signal-regulated kinase; OSR1, oxidative stress response kinase-1; PP1 $\gamma$ , protein phosphatase-1 $\gamma$ ; SPAK, STE20/SPS1-related proline alanine-rich kinase; WNK, with-no-K[Lys] kinase.

The online version of this article contains supplemental material.

coexpressed ion cotransporters or ion channels. These have thus far revealed that WNK isoforms have effects on the activity and/or membrane expression of the thiazide-sensitive  $\text{Na}^+:\text{Cl}^-$  cotransporter (NCC), the bumetanide-sensitive  $\text{Na}^+:\text{K}^+:\text{2Cl}^-$  cotransporter-1/2 (NKCC1/2), the  $\text{K}^+:\text{Cl}^-$  cotransporter-2, the  $\text{Cl}^-:\text{HCO}_3^-$  exchanger, the inwardly rectifying  $\text{K}^+$  channel, the epithelial  $\text{Na}^+$  channel, the tight junction claudin proteins, and the transient receptor potential vanilloid-4  $\text{Ca}^{2+}$  channel (for reviews see Delaloy et al., 2005; Kahle et al., 2005; Gamba, 2006).

Recent findings indicate that the protein kinases WNK1 and -4 interact with high affinity with the protein kinases STE20/SPS1-related proline alanine-rich kinase (SPAK) and the oxidative stress response kinase-1 (OSR1; Piechotta et al., 2003; Vitari et al., 2005; Gagnon et al., 2006). These observations were followed by the finding that WNK1 and -4 could phosphorylate and activate SPAK and OSR1 *in vitro* (Moriguchi et al., 2005; Vitari et al., 2005; Anselmo et al., 2006). SPAK and OSR1 are phosphorylated by WNK1/WNK4 at a Thr residue located within the T-loop (Thr233-SPAK and Thr185-OSR1) as well as at a conserved noncatalytic Ser residue (Ser373-SPAK and Ser325-OSR1) lying within a region termed the S-motif (Vitari et al., 2005). Mutational analysis indicated that phosphorylation of the T-loop rather than the S-motif was required for the activation of SPAK and OSR1 by WNK1 (Vitari et al., 2005). SPAK and OSR1 were originally identified through their ability to interact, phosphorylate, and activate NKCC1 (Piechotta et al., 2002; Dowd and Forbush, 2003) and may also regulate NCC (Pacheco-Alvarez et al., 2006). SPAK and OSR1 are 68% identical in sequence and possess a highly similar kinase catalytic domain as well as a conserved C-terminal (CCT) domain, which interacts with RFXV/I motifs present in both WNK isoforms as well as NKCC1 (Piechotta et al., 2002; Moriguchi et al., 2005; Gagnon et al., 2006; Vitari et al., 2006). The activity and phosphorylation of NKCC family cotransporters is stimulated by hyperosmotic stress (Lytle and Forbush, 1992; Kurihara et al., 1999; Darman and Forbush, 2002), conditions that have also been reported to enhance WNK1 activity (Xu et al., 2002; Lenertz et al., 2005) and induce phosphorylation of NKCC1 at the sites targeted by SPAK/OSR1 *in vitro* (Vitari et al., 2006). In this study, we investigate the mechanism by which WNK1 as well as its substrates SPAK/OSR1 are regulated by hyperosmotic stress.

## Results

### Activation of WNK1 by hyperosmotic stress

It has been reported that hyperosmotic stress stimulates WNK1 activity (Xu et al., 2002; Lenertz et al., 2005). As a prelude to investigating the mechanism by which WNK1 is regulated, we further assessed the activity of endogenous WNK1 in 293 cells. We found that WNK1 immunoprecipitated from sorbitol-treated cells phosphorylated OSR1 at an approximately threefold higher rate than WNK1 derived from nontreated cells (Fig. 1 A). Consistent with WNK1 mediating this phosphorylation, no phosphorylation of OSR1 was detected when a

mutated form of OSR1 in which the T-loop (Thr185) and S-motif (Ser325) sites phosphorylated by WNK1 were changed to Ala or when preimmune antibody was used instead of the specific anti-WNK1 antibody in the immunoprecipitation step (Fig. 1 A). A dose-dependent increase in WNK1 activity was observed by treatment with 0.1–1.0 M sorbitol, resulting in up to a fivefold increase of WNK1 activity (Fig. 1 B). Activation of WNK1 by 0.5 M sorbitol was detected within 0.5 min, with maximal activation being reached within 1–2 min, which was sustained for 80 min (Fig. 1 C). Consistent with hyperosmotic stress activating WNK1, treatment of cells with increasing concentrations of NaCl also induced activation of WNK1, which was detectable at 50 mM and maximal at 0.15 M (Fig. 1 D). Similarly, treatment of cells with 0.5 M KCl led to a threefold increase of WNK1 activity (Fig. 1 E). We next explored whether WNK1 was activated by other stimuli, namely, serum, IGF-1, phorbol ester (TPA), oxidative stress ( $\text{H}_2\text{O}_2$ ), hypotonic stress (medium diluted twofold in  $\text{H}_2\text{O}$ ), an NKCC1/2 inhibitor (bumetanide),  $\text{TNF}\alpha$ , a tyrosine phosphatase inhibitor (pervanadate), or a serine/threonine phosphatase inhibitor (calyculin A). These treatments failed to induce activation of WNK1 under conditions in which they triggered activation of other signaling pathways (Fig. 1 E). As 0.5 M sorbitol stimulated the extracellular signal-regulated kinase (ERK) 1/2, p38, and JNK protein kinases (Fig. 1 E), we investigated whether these enzymes might be involved in the activation of WNK1. Treatment of cells with the MEK inhibitor PD184352 (Fig. 1 F) or U0126 (not depicted) abolished ERK activation by sorbitol, without affecting WNK1 activation. The p38 inhibitor SB203580 and high concentrations of BIRB0796 that inhibit all p38 and JNK isoforms (Kuma et al., 2005) also failed to prevent activation of WNK1 by sorbitol (Fig. 1 F). Consistent with p38 and JNK not regulating WNK1, anisomycin that potently stimulates p38 and JNK failed to activate WNK1 (Fig. 1 F).

### Hyperosmotic stress induces phosphorylation of WNK1 at multiple residues

Despite the large size of WNK1 (~250 kD), we consistently observed a reduction in the electrophoretic mobility of endogenous WNK1 isolated from sorbitol-treated cells on a polyacrylamide gel (Fig. 2 A). To assess whether this was due to enhanced phosphorylation, 293 cells were labeled with  $^{32}\text{P}$ -orthophosphate and endogenous WNK1 was immunoprecipitated from control and sorbitol-treated cells. Electrophoresis on a polyacrylamide gel revealed a Coomassie-stained band at ~250 kD that was identified as WNK1 by mass spectrometry (Fig. 2 B). Autoradiographic analysis of the gel revealed that phosphorylation of WNK1 was stimulated by sorbitol (Fig. 2 B). The  $^{32}\text{P}$ -labeled WNK1 from control and sorbitol-treated cells was digested with trypsin, and the resulting peptides were chromatographed on a  $\text{C}_{18}$  column. Sorbitol substantially increased the abundance of several  $^{32}\text{P}$ -labeled peptides (Fig. 2 C). All phosphopeptides were subjected to mass spectrometry and some of them to solid phase Edman sequencing analysis, which enabled us to identify five sites of phosphorylation (Fig. 2 C). Phosphorylation of two sites, Ser1261 and

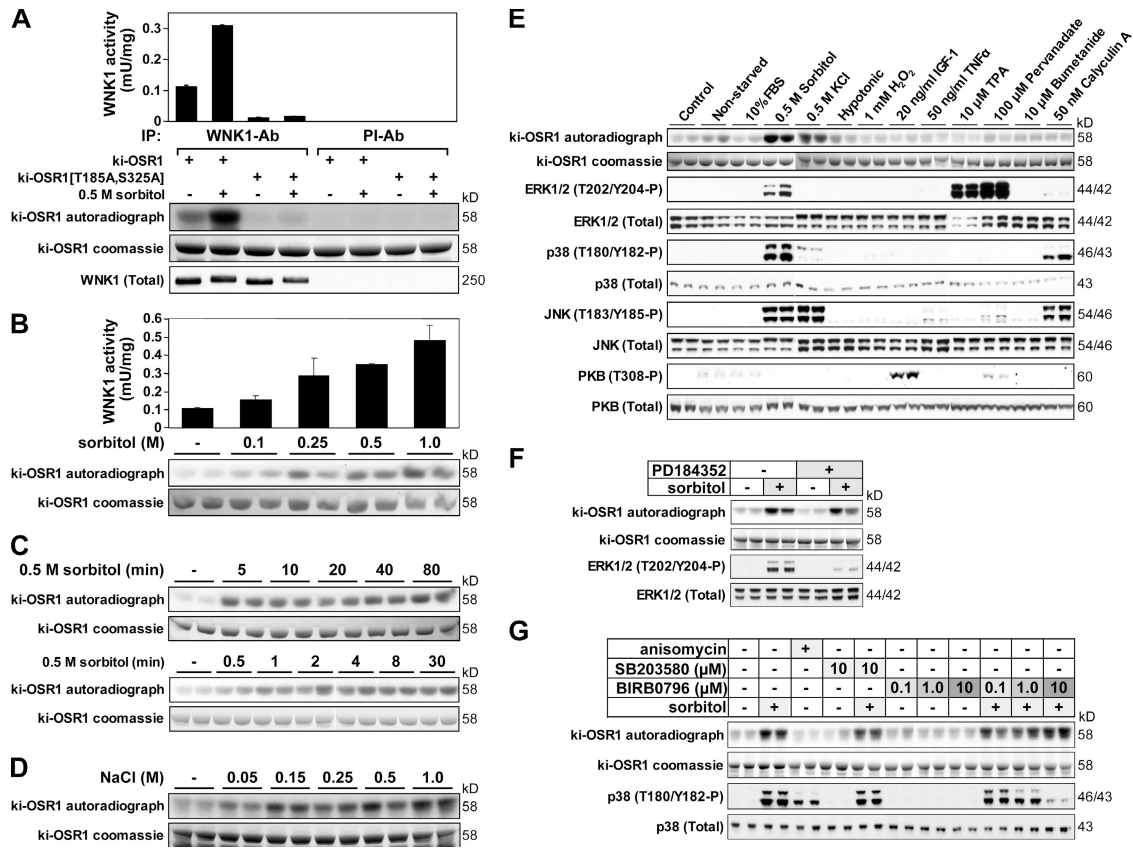


**Figure 1. Characterization of WNK1 activity.** (A) 293 cells were stimulated with 0.5 M sorbitol for 30 min. Immunoprecipitations from the cell lysates were performed with the anti-WNK1(CT) antibody (WNK1-Ab) or the preimmune antibody (PI-Ab), and the kinase activity of the immunoprecipitates was measured using either kinase-inactive OSR1[D164A] (ki-OSR1) or a mutant of OSR1 in which the WNK1 phosphorylation sites have been changed to Ala [ki-OSR1[T185A,S325A]]. Phosphorylation of OSR1 was analyzed after electrophoresis on a polyacrylamide gel, Coomassie blue staining (middle), and autoradiography (top). The incorporation of phosphate was also quantified on a Wallac Scintillation Counter (graph), and results are presented as the mean specific activity  $\pm$  SD for duplicate samples. Similar results were obtained in at least two experiments. (B) As above, except that 293 cells were stimulated with the indicated concentrations of sorbitol for 30 min. (C) As in A, except that 293 cells were stimulated with 0.5 M sorbitol for the indicated times. (D) As in B, except that 293 cells were stimulated with the indicated concentrations of NaCl for 30 min. (E) As in B, except that 293 cells were deprived of serum for 16 h and treated with the indicated stimuli for 30 min. For the hypotonic stimulation, the cell medium was diluted twofold in H<sub>2</sub>O. Cell lysates were also immunoblotted with the indicated antibodies. (F) As in E, except that cells were preincubated with 2  $\mu$ M PD184352 for 30 min before stimulation with 0.5 M sorbitol for 30 min. (G) As in E, except that cells were either left untreated (–) or preincubated (+) with 10  $\mu$ M SB203580 or the indicated concentrations of BIRB0796 for 30 min and then stimulated with 10  $\mu$ g/ml anisomycin or 0.5 M sorbitol for an additional 30 min (in the continued absence or presence of inhibitor).

Ser 2372, was stimulated by treatment of cells with sorbitol, whereas Ser2012, Ser2029, and Ser2032 were phosphorylated at similar levels in WNK1 isolated from control and sorbitol-stimulated cells.

As several of the phosphopeptides observed in the <sup>32</sup>P-cell-labeling experiments presented in Fig. 2 B were not present at sufficient levels to enable phosphorylation site assignment, we undertook a mass spectrometry phosphopeptide mapping analysis of a larger amount of endogenous WNK1 immunoprecipitated from unlabeled control and sorbitol-treated 293 cells (Fig. 2 D). The immunoprecipitated WNK1 was digested with trypsin, and the resulting peptides were subjected to liquid chromatography/mass spectrometry with precursor ion scanning on a Q-TRAP mass spectrometer, which enabled us to assign five residues (Ser15, Ser167, Ser382, Ser1261, and Thr1848) whose phosphorylation was markedly enhanced by treatment of cells with sorbitol (Fig. 2 D). One of these sites, Ser382, which lies within the T-loop of the WNK1 catalytic domain,

has been reported to be an autophosphorylation site on WNK1 catalytic domain expressed in *Escherichia coli* (Xu et al., 2002). The location of all the phosphorylation sites identified within WNK1 and the amino acid sequences surrounding these sites are illustrated in Fig. 2 (E and F).

### Phosphorylation mediates WNK1 activation induced by hyperosmotic stress

To verify whether the activity of WNK1 was influenced by its phosphorylation state, we incubated WNK1 isolated from control and sorbitol-treated 293 cells with the serine/threonine protein phosphatase-1 $\gamma$  (PP1 $\gamma$ ) and assessed its activity. We observed that incubation with PP1 $\gamma$  substantially decreased both the basal and sorbitol-stimulated activity of WNK1 and also increased WNK1 electrophoretic mobility (Fig. 2 G). Microcystin-LR, a toxin that specifically inhibits serine/threonine phosphatases, prevented PP1 $\gamma$ -induced inactivation as well as the increase in WNK1 electrophoretic mobility (Fig. 2 G).



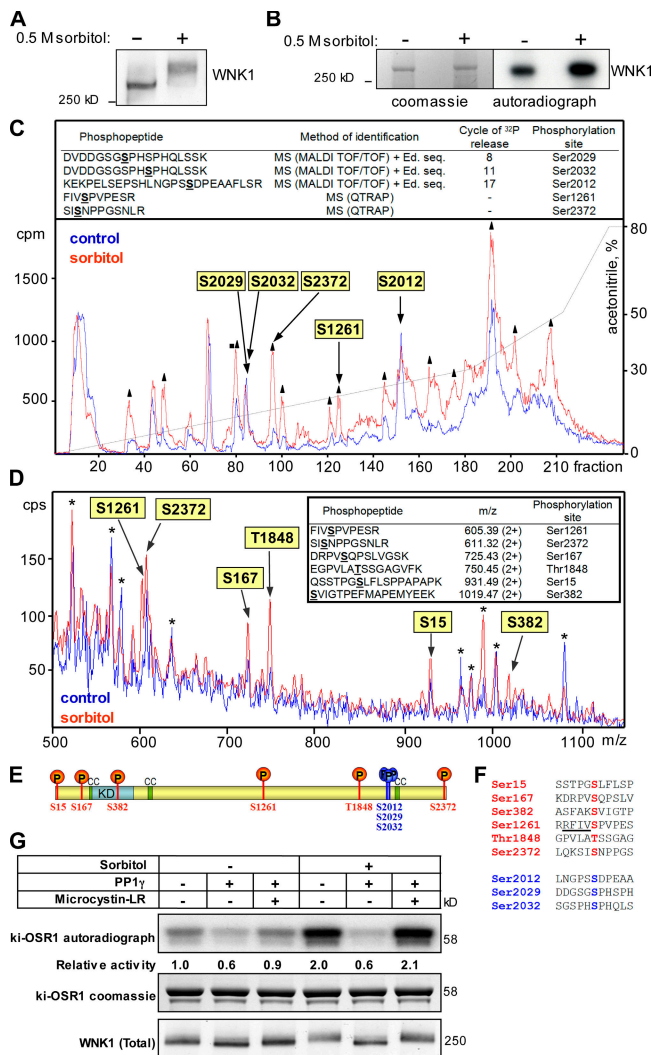


**Figure 2. Identification of phosphorylation sites on WNK1.** (A) Endogenous WNK1 was immunoprecipitated from control or sorbitol-stimulated (0.5 M for 30 min) 293 cells and subjected to immunoblot analysis with the anti-WNK1 antibody. (B) 293 cells were labeled with <sup>32</sup>P and left untreated or stimulated with 0.5 M sorbitol for 20 min. The endogenously expressed WNK1 was immunoprecipitated and subjected to electrophoresis on a polyacrylamide gel, which was then stained with colloidal Coomassie blue and autoradiographed. The Coomassie-stained bands migrating with the expected molecular mass of WNK1 were excised from the gel and digested with trypsin, and a small aliquot (<1%) was analyzed by MALDI TOF/TOF mass spectrometry and confirmed to contain WNK1 tryptic peptides. (C) The remaining WNK1 tryptic peptides were chromatographed on a reverse-phase HPLC Vydac C18 column. The figure shows <sup>32</sup>P radioactivity versus HPLC fraction number for the phosphopeptides derived from WNK1 isolated from control (blue) or sorbitol-stimulated (red) cells. A similar HPLC profile was obtained in two separate experiments. All major <sup>32</sup>P-labeled peptides were analyzed by MALDI TOF/TOF and 4000 Q-TRAP mass spectrometry. This resulted in the identification of five phosphopeptides indicated by the yellow boxes, and the sites of phosphorylation of the phosphopeptides identified by MALDI TOF/TOF were confirmed by solid-phase Edman sequencing (Ed. seq.). There is mass spectrometry evidence that the peptide labeled with a solid square is a diphospho form of the DVDDGSGSPHSPHQLSSK peptide that may be labeled at both Ser2029 and Ser2032. (D) WNK1 was immunoprecipitated from 100 mg of unlabeled 293 cell lysate derived from control or sorbitol-stimulated (0.5 M, for 30 min) cells. The samples were subjected to electrophoresis on a polyacrylamide, and the Coomassie-stained bands corresponding to WNK1 were excised and digested with trypsin. Phosphopeptides were identified by combined liquid chromatography-mass spectrometry and tandem mass spectrometry analysis. The figure shows the signal intensity (cps, counts of

## Phosphorylation of Ser382 mediates activation of WNK1

We observed that an N-terminal fragment of WNK1 encompassing residues 1–667 retained the property of becoming activated after stimulation of 293 cells with sorbitol (Fig. 3). Mutation of Ser382 that lies within the T-loop of WNK1 to Ala prevented activation of WNK1 by sorbitol treatment (Fig. 3 A), consistent with the previous report that this mutation inhibited WNK1 activity expressed in *E. coli* (Xu et al., 2002). Mutation of Ser382 to Glu enhanced the basal activity of WNK1[1–667] to a level that was over eightfold higher than that observed for wild-type WNK1[1–667] isolated from untreated cells (Fig. 3 A). The activity of the WNK1[S382E, 1–667] mutant was not enhanced by sorbitol stimulation.

Sorbitol markedly increased recognition of WNK1[1–667] by a phospho-Ser382 antibody that we generated (Fig. 3 A). Consistent with this antibody being specific, mutation of Ser382 to Ala abolished its recognition of WNK1 (Fig. 3 A). We also observed that sorbitol treatment induced Ser382 phosphorylation of a catalytically inactive WNK1[D368A, 1–667] mutant to the same extent as the catalytically active WNK1[1–667] fragment (Fig. 3 A), indicating that phosphorylation of WNK1 at Ser382 was not mediated by intramolecular autophosphorylation.

## WNK1 can autophosphorylate at Ser382

To determine whether WNK1 possesses the intrinsic ability to autophosphorylate on Ser382, we expressed wild-type WNK1[1–661] or kinase-inactive WNK1[D368A, 1–661] in *E. coli*. Consistent with previous work (Xu et al., 2002), we observed that the wild-type WNK1[1–661] was heavily phosphorylated at Ser382 and also possessed a high specific activity of 5.2 U/mg (Fig. 3 B). The activity of *E. coli* expressed WNK1[1–661] was much higher than that of the WNK1[1–667] fragment isolated from sorbitol-stimulated 293 cells, which had a specific activity of only ~0.13 U/mg (Fig. 3). We observed that the kinase-inactive WNK1[D368A, 1–661] mutant expressed in *E. coli* was not phosphorylated at Ser382 (Fig. 3 B). Moreover, the WNK1[S382A, 1–661], WNK1[S382E, 1–661], and WNK1[S382D, 1–661] mutants expressed in *E. coli* possessed low activities of 0.15, 0.66, and 0.26 U/mg, respectively (Fig. 3 B). Incubation of wild-type WNK1[1–661] with MgATP in vitro did not further increase phosphorylation of Ser382 (Fig. 3 C).

ions per second detected) versus the ion distribution (m/z) for the phosphopeptides derived from WNK1 isolated from control (blue) or sorbitol-stimulated (red) cells. We were unable to identify the peptides marked with asterisks. (E) Illustration of the location of the identified sorbitol-induced (red) and constitutive (blue) sites of phosphorylation within the WNK1 protein. KD, kinase domain (residues 221–479); CC, coiled-coil domains (residues 189–221, 566–595, and 2072–2101). (F) The amino acid sequence surrounding each of the phosphorylation sites identified in human WNK1 is presented. The RFXV/I motif lying adjacent to the site of phosphorylation of Ser1261 is underlined. (G) WNK1 immunoprecipitates derived from control and sorbitol-stimulated (0.5 M, 30 min) 293 cells were incubated with PP1γ, in the presence or absence of microcystin-LR, an inhibitor of Ser/Thr protein phosphatases, and assayed as described in the legend to Fig. 1. The results are presented as relative activity compared with that of WNK1 isolated from untreated cells and not treated with PP1γ, which was given a value of 1.0. An aliquot of the reaction mixtures was also immunoblotted with the anti-WNK1 antibody. Similar results were obtained in two separate experiments conducted in duplicate.

### Phosphorylation of Ser1261 may inhibit WNK1 interaction with SPAK/OSR1

As outlined in the introduction, WNK1 interacts with its substrates SPAK and OSR1 through RFXV/I motifs. Interestingly, the site of phosphorylation, Ser1261, is located adjacent to such a motif (Fig. 2 E), suggesting that phosphorylation of Ser1261 might influence the ability of WNK1 to bind SPAK and OSR1. To investigate this, we generated biotinylated peptides that encompass residues surrounding Ser1261 in its phosphorylated or nonphosphorylated form. These were conjugated to streptavidin–Sepharose and tested for ability to affinity purify endogenously expressed SPAK and OSR1 from 293 cell extracts. The nonphosphorylated Ser1261 peptide interacted with SPAK and OSR1 to a markedly greater extent than the

phosphorylated peptide (Fig. 4 A). Using a surface plasmon resonance binding assay, we also observed that the nonphosphorylated Ser1261 peptide interacted with a dissociation constant of  $\sim 40$  nM with the isolated CCT domain of OSR1, whereas the phosphorylated Ser1261 peptide bound to OSR1 with a markedly lower affinity (Fig. 4 B).

### Hyperosmotic stress induces activation and phosphorylation of SPAK and OSR1

We next studied whether the downstream substrates of WNK1, SPAK and OSR1, were activated by hyperosmotic stress in HeLa and 293 cells. Endogenous SPAK and OSR1 were immunoprecipitated from control and sorbitol-treated cells with an antibody that immunoprecipitates both proteins and assayed using a peptide substrate termed CATCHtide (Vitari et al., 2006). The activity of SPAK/OSR1 was increased approximately five-fold by sorbitol stimulation of HeLa cells (Fig. 5 A, top) and approximately fourfold in 293 cells (Fig. S1, available at <http://www.jcb.org/cgi/content/full/jcb.200605093/DC1>). This is consistent with previous reports that these enzymes are activated by sorbitol (Chen et al., 2004; Anselmo et al., 2006). We raised phosphospecific antibodies that recognize the T-loop and S-motif residues on SPAK and OSR1 phosphorylated by WNK1. The sequences surrounding these sites are almost identical in SPAK and OSR1 (Vitari et al., 2005), suggesting that

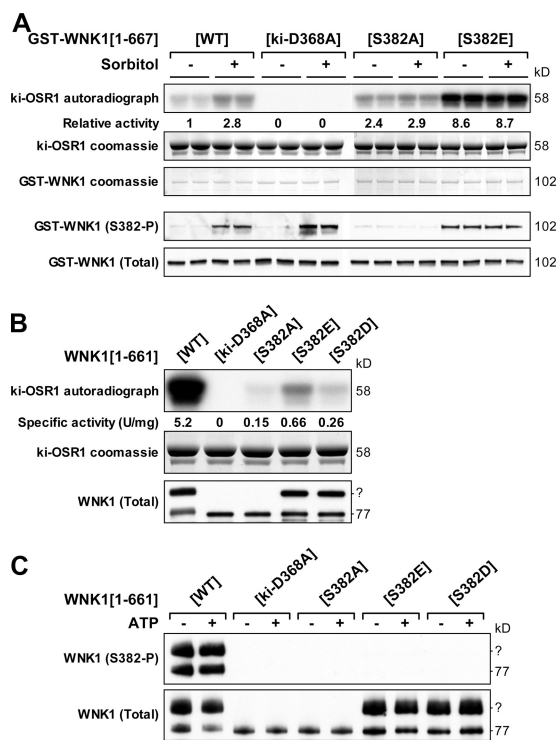


**Figure 3. Evidence that phosphorylation of Ser382 mediates WNK1 activation.** (A) 293 cells were transfected with constructs encoding the indicated forms of GST-WNK1[1–667]. 36 h after transfection, the cells were left untreated or treated with 0.5 M sorbitol for 30 min and lysed. GST-WNK1 was affinity purified on glutathione–Sepharose and assayed as described in the legend to Fig. 1. The results are presented as the mean relative activity  $\pm$  SD compared with the activity observed for wild-type WNK1[1–667] isolated from untreated cells, which is given a value of 1.0 (its specific activity was 0.13 U/mg). Similar results were obtained in at least two experiments conducted in duplicate. Cell lysates were immunoblotted with the indicated antibodies. (B) The indicated forms GST-WNK1[1–661] were expressed in *E. coli*, purified, and assayed. Results are presented as the mean specific activity for duplicate samples, and similar results were obtained in at least two experiments. An aliquot of the reaction mixtures was also immunoblotted with the anti-WNK1 antibody. The WNK1[1–661], WNK1[S382E, 1–661], or WNK1[S382D, 1–661] fragments migrate for unknown reasons as a doublet band on SDS-PAGE, whereas the WNK1[D368A, 1–661] or WNK1[S382A, 1–661] migrate as a single band with the expected molecular mass of 77 kD. The question mark indicates that the identity of the slower migrating WNK1 band is uncertain. (C) The indicated forms of WNK1 purified from *E. coli* were incubated in the absence (–) or presence (+) of 0.1 mM ATP and 10 mM Mg for 1 h before immunoblotting with the indicated antibodies.

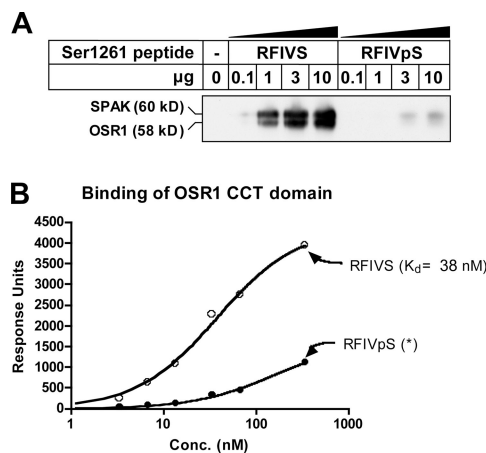


**Figure 4. Evidence that phosphorylation of Ser1261 inhibits binding of WNK1 to SPAK/OSR1.** (A) The indicated amounts of a biotinylated peptide encompassing Ser1261 of WNK1 (biotin-AGRRFIVSPVPESRL) or the phosphorylated form of this peptide (AGRRFIVpSPVPESRL) were conjugated to streptavidin–Sepharose and incubated with 1 mg of 293 cell lysate. After isolation and washes of the beads, the samples were electrophoresed on a polyacrylamide gel and immunoblotted with an antibody recognizing both SPAK and OSR1. (B) The binding of bacterially expressed purified forms of the OSR1 CCT domain (residues 429–527) to the biotinylated peptides used above was analyzed using BiaCore. The analysis was performed over a range of protein concentrations (6.8–340 nM), and the response level at steady state was plotted against the log of the protein concentration. The dissociation constant was calculated by fitting the data to the formula ( $Y = B_{max} * X / [K_d + X]$ ) using GraphPad 4 software, which describes the binding of a ligand to a receptor that follows the law of mass action.  $B_{max}$  is the maximal binding, and  $K_d$  is the concentration of ligand required to reach half-maximal binding. X and Y correspond to the protein concentration and the response units, respectively. The asterisk indicates that binding to the phosphorylated peptide was too weak to reliably calculate a dissociation constant.

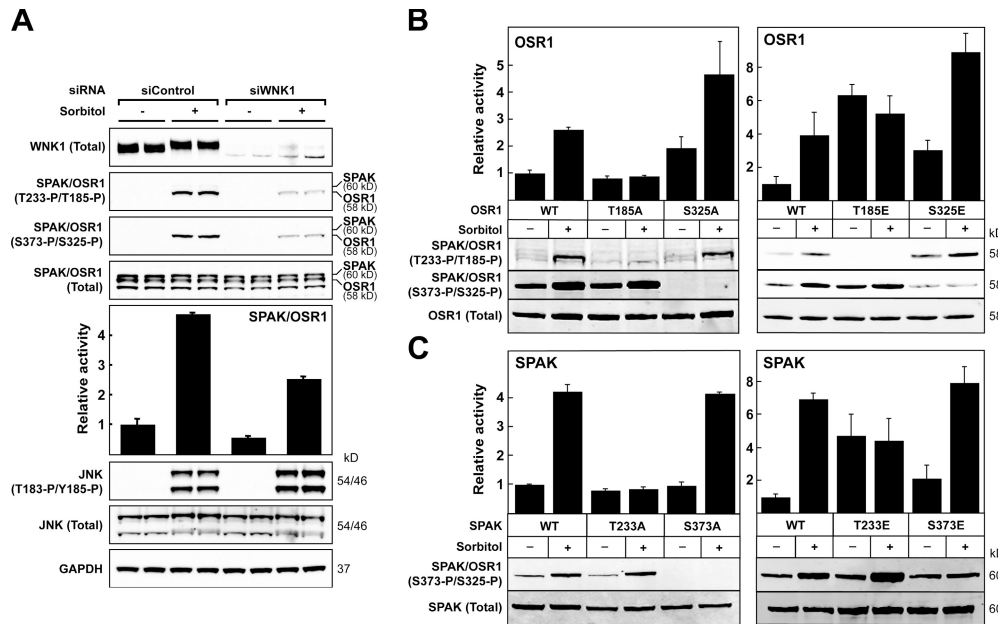


**Figure 5. Hyperosmotic stress leads to WNK1-mediated activation and phosphorylation of SPAK and OSR1.** (A) HeLa cells were transfected with a control siRNA duplex or a siRNA duplex targeting human WNK1 as described in Materials and methods. 48 h after transfection, cells were either left untreated or stimulated with 0.5 M sorbitol for 30 min. Endogenously expressed SPAK and OSR1 were immunoprecipitated from the cell extracts using an antibody that immunoprecipitates both SPAK and OSR1, and their activity was assayed using the CATCHtide peptide substrate (Vitari et al., 2006). Results are presented as the mean relative activity  $\pm$  SD compared with that observed for SPAK/OSR1 isolated from untreated cells that have been transfected with the control siRNA duplex, which was given a value of 1.0. Total cell extracts (20  $\mu$ g) were also immunoblotted with the indicated antibodies. Similar results were obtained in three separate experiments conducted in duplicate. (B and C, top) 293 cells were transfected with constructs encoding the wild-type and indicated mutant forms of GST-OSR1 (B) or GST-SPAK (C). 36 h after transfection, the cells were left untreated or treated with 0.5 M sorbitol for 30 min and lysed. GST-OSR1/SPAK forms were affinity purified on glutathione-Sepharose and assayed using a fragment of NKCC1 encompassing residues 1–260. Results are presented as the mean relative activity  $\pm$  SD compared with the activity observed for wild-type OSR1/SPAK isolated from untreated cells, which is given a value of 1.0. Similar results were obtained in at least two experiments conducted in triplicate. (bottom) The cell lysates were also immunoblotted with the indicated phosphospecific antibodies as well as anti-GST antibody to detect GST-OSR1/SPAK proteins.

the T-loop and S-motif phosphospecific antibodies should recognize the phosphorylated forms of both SPAK and OSR1. The specificity of the antibodies was confirmed by overexpressing OSR1 (Fig. 5 B) or SPAK (Fig. 5 C) in 293 cells and finding that mutation of the T-loop or S-motif residues to Ala abolished antibody recognition. Using these antibodies, we demonstrated that sorbitol treatment markedly stimulated the phosphorylation of endogenously expressed SPAK and OSR1 at both the T-loop and S-motif in HeLa cells (Fig. 5 A) as well as in 293 cells (Fig. S1). Sorbitol also induced a decrease in the electrophoretic mobility of endogenous SPAK. Studying overexpressed OSR1 (Fig. 5 B) and SPAK (Fig. 5 C) in 293 cells, we observed that mutation of the T-loop, but not the S-motif, to Ala, inhibited sorbitol-induced activation of these enzymes. We also found that mutation of the T-loop residue to Glu markedly increased the basal activity of OSR1 and SPAK and the activity of these mutants was not further increased by sorbitol treatment of cells. Mutation of the S-motif to Glu moderately enhanced basal and sorbitol-stimulated OSR1 (Fig. 5 B) and SPAK (Fig. 5 C) activity.

#### Evidence that WNK1 regulates SPAK and OSR1 activity and phosphorylation in vivo

We next investigated the effect of depleting the levels of endogenous WNK1 using a siRNA duplex targeting WNK1 that reduces expression >90% (Fig. 5 A). Under these conditions,

sorbitol-induced phosphorylation of the T-loop and S-motif of SPAK and OSR1 were markedly reduced. Depletion of WNK1 also inhibited the basal as well as sorbitol-induced SPAK/OSR1 activity by >50% without affecting sorbitol-induced phosphorylation of JNK isoforms at their T-loop residues (Fig. 5 A).

#### Hyperosmotic stress induces redistribution of WNK1 to intracellular vesicles colocalizing with clathrin

We also studied the localization of GFP-WNK1 (Fig. 6) that was stably expressed at a similar level to that of endogenous WNK1 (Vitari et al., 2004) as well as the localization of endogenous WNK1 in 293 cells (Fig. 7). In unstimulated cells, WNK1 was diffusely localized throughout the cytosol (Figs. 6 and 7, panel 1), but after treatment with 0.2 M sorbitol for only 1 min, WNK1 was strikingly observed on discrete intracellular structures. Colocalization experiments revealed that both GFP-WNK1 and endogenous WNK1 colocalized with clathrin (Figs. 6 and 7, panel 2) as well as AP-1 (Figs. 6 and 7, panel 3), which is an adaptor for clathrin and is recruited to budding vesicles at the TGN and endosomes (Hirst and Robinson, 1998). Partial colocalization between GFP-WNK1 and the TGN46 integral membrane protein that is predominantly localized to the TGN was also observed (Fig. 6, panel 4). In contrast, WNK1 did not colocalize with the early endosomal markers EEA1 (Mu et al., 1995) and Hrs (Raiborg et al., 2001) or the late endosome and



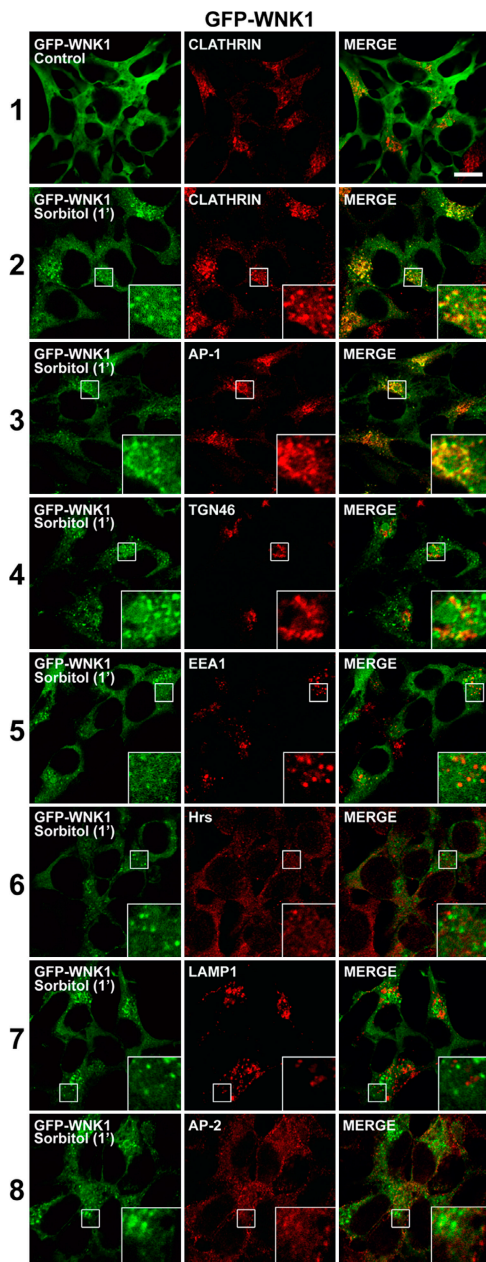


Figure 6. **Translocation of GFP-WNK1 to clathrin-coated vesicles after hyperosmotic stress.** 293 cells stably expressing GFP-WNK1 were left unstimulated (control) or stimulated with 0.2 M sorbitol for 1 min, before fixation. Cells were immunostained in the red channel with antibodies recognizing clathrin, AP-1, TGN46, EEA1, Hrs, LAMP1, or AP-2 and in the green channel for GFP-WNK1. Fluorescent imaging was performed on a confocal microscope. Similar results were obtained in two independent experiments. Bar, 10  $\mu$ m.

lysosome marker LAMP1 (Rohrer et al., 1996; Figs. 6 and 7). Nor did it colocalize with the AP-2 adaptor (Figs. 6 and 7), which plays a central role in clathrin-mediated endocytosis by linking transmembrane receptors to be internalized to the clathrin lattice (Hirst and Robinson, 1998). We next investigated the redistribution of stably expressed GFP-WNK1 in living 293 cells using time-lapse microscopy (Fig. 8 and Videos 1 and 2, available at <http://www.jcb.org/cgi/content/full/jcb.200605093/DC1>). The redistribution of GFP-WNK1 to intracellular vesicles after

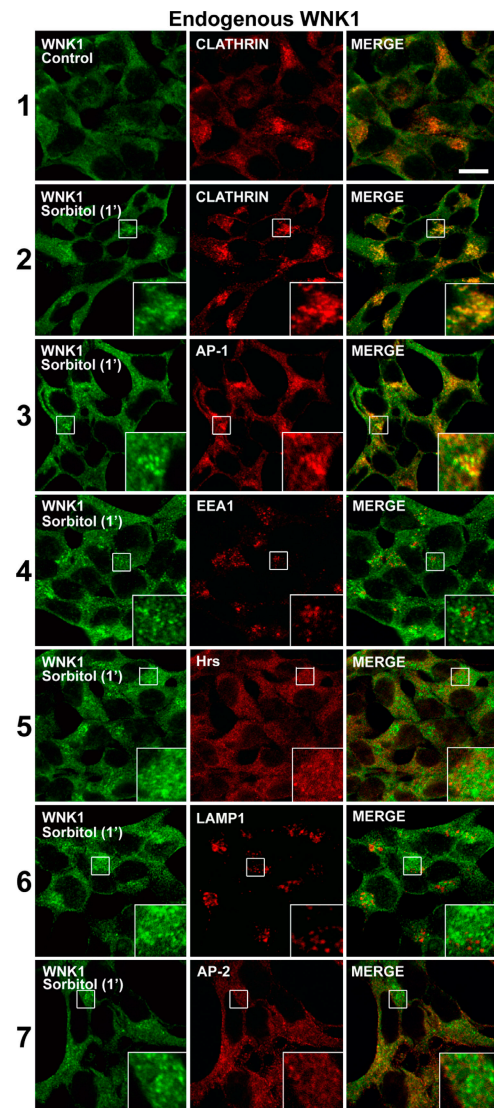


Figure 7. **Translocation of endogenous WNK1 to clathrin-coated vesicles after hyperosmotic stress.** 293 cells were left unstimulated (control) or stimulated with 0.2 M sorbitol for 1 min, before fixation. Cells were immunostained in the red channel with antibodies recognizing clathrin, AP-1, EEA1, Hrs, LAMP1, or AP-2 and in the green channel with the anti-WNK1 antibody to detect endogenous WNK1. Fluorescent imaging was performed on a confocal microscope. Similar results were obtained in two independent experiments. Bar, 10  $\mu$ m.

sorbitol (Video 1) or NaCl (Video 2) treatment was rapid and observed within  $\sim$ 0.5 min, the earliest time point that we could monitor (Fig. 8 A). Frames of the video were taken every 2 s, and substantial movement of some of the GFP-WNK1 localized was observed within a 10–30-s time frame (Videos 1 and 2 and Figs. S2 and S3). This effect was reversible, as removal of sorbitol or NaCl resulted in WNK1 becoming diffusely localized in the cytosol within 2 min (Fig. 8 B). We also undertook an experiment of FRAP to monitor the dynamics of WNK1 movement within the cells. In sorbitol- or NaCl-treated cells (Fig. 8 C), WNK1 became redistributed to the photobleached area within 2 min. This was slower than in untreated cells, where the recovery occurred within 0.5 min (unpublished data).

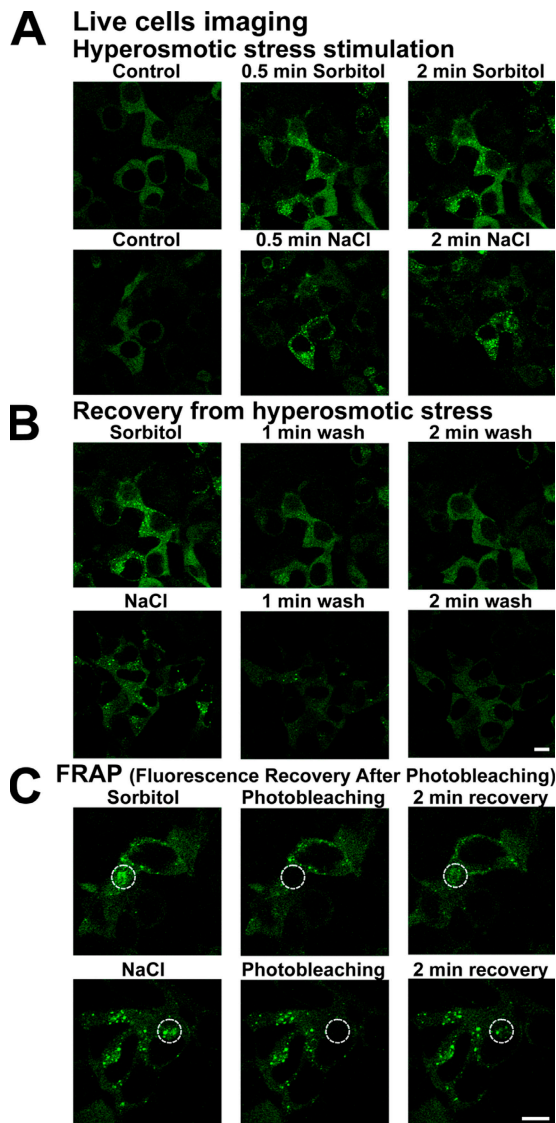


Figure 8. **Localization of GFP-WNK1 in living cells.** (A) 293 cells stably expressing GFP-WNK1 were mounted in a heated chamber for live-cell fluorescent imaging using a confocal microscope. Images were collected every 10 s. Before stimulation, cells were visualized for 2 min, and the cells labeled control correspond to a representative image of the cells during this period. After 2 min, the medium was exchanged with prewarmed medium containing either 0.2 M sorbitol (top) or 0.2 M NaCl (bottom), and the cells were observed for a further 5 min. An image of the cells after 0.5 and 2 min is shown. (B) As described in A, except that after imaging the sorbitol (top) or NaCl-treated (bottom) cells for 5 min, the medium was exchanged twice with prewarmed DME not containing sorbitol or NaCl and the cells were imaged for a further 5 min. The image of the cells after 1 and 2 min is shown. (C) As in A, except that the region indicated by the dotted circle was photobleached and cells were observed for a further 5 min, imaging every 10 s. The image of the cells after 2 min is shown. The photobleaching experiment was performed in duplicate, and at least four separate cells were visualized in each experiment. A representative cell from these experiments is shown. Bars, 10  $\mu\text{m}$ .

#### The noncatalytic C-terminal domain of WNK1 mediates translocation to intracellular vesicles

We observed that the C-terminal noncatalytic domain of WNK1 comprising residues 1504–2382 fused to GFP redistributed to intracellular vesicles after sorbitol stimulation, similar to

full-length GFP-WNK1 (Fig. 9). In contrast, the N-terminal fragment (residues 1–667) comprising the catalytic domain remained diffusely localized throughout the cytoplasm after sorbitol stimulation.

## Discussion

Our findings are consistent with previous reports (Xu et al., 2002; Lenertz et al., 2005) suggesting that endogenously expressed WNK1 is specifically activated by hyperosmotic conditions (sorbitol, NaCl, and KCl) and not by other stresses ( $\text{H}_2\text{O}_2$ , anisomycin, and phosphatase inhibitors), growth factors, cytokines, phorbol esters, or the diuretic hypotensive agent bumetanide (Fig. 1). The activation of WNK1 by sorbitol is rapid and observed within 0.5 min, the earliest time point that we can practically investigate. Our data indicate that hyperosmotic stress activates WNK1 by stimulating its phosphorylation as incubation of WNK1 with  $\text{PP1}\gamma$  lead to a decrease in its activity. Phosphopeptide mapping resulted in the identification of six residues on endogenous WNK1 whose phosphorylation is stimulated with sorbitol (Fig. 2). Two of these sites are located N-terminal to the kinase domain (Ser15 and Ser167), one within the T-loop of the kinase domain (Ser382), and the other three sites are within the C-terminal noncatalytic region (Ser1261, Thr1848, and Ser2372). In addition, we have identified three other phosphorylation sites within the C-terminal region of WNK1 (Ser2012, Ser2029, and Ser2032) that are constitutively phosphorylated. We cannot rule out the possibility that there are additional phosphorylation sites on WNK1 that we have not been able to identify. Apart from Ser15, all the phosphorylation residues identified are conserved in mouse and rat WNK1. In *Drosophila melanogaster* WNK1, Ser382 and Ser2372 are conserved, whereas in *C. elegans* WNK1, only Ser382 is conserved. The only phosphorylation site that is present in all human WNK isoforms is Ser382, and the residues surrounding this site are also identical in all WNK isoforms. Ser2372 is found in WNK2 and -3, but not WNK4. Alignment of the sequences surrounding the WNK1 phosphorylation sites (Fig. 2 F) indicates that they are quite distinct, suggesting that different upstream kinases may be phosphorylating these residues in vivo. The only similarity between three of the phosphorylation sites (Ser1261, Ser2029, and Ser2032) is that they possess a proline residue following the site of phosphorylation. It would be interesting to investigate whether these residues were phosphorylated by a proline-directed kinase, such as an isoform of p38 or JNK. If this was the case, the phosphorylation of these sites may not be regulating WNK1 activity, as inhibitors of p38–JNK–ERK pathways did not prevent WNK1 activation (Fig. 1 F).

Our results suggest that phosphorylation of Ser382 is required for sorbitol-induced activation of WNK1, as mutation of Ser382 to Ala prevented WNK1 activation by sorbitol, whereas mutation of Ser382 to Glu to mimic phosphorylation increased activity of WNK1 and prevented further activation by sorbitol (Fig. 3). The conservation of Ser382 in all species of WNK isoforms is consistent with the notion that phosphorylation of this residue plays a crucial role in controlling the activity of WNK isoforms. It was previously reported that the isolated catalytic



domain of WNK1 encompassing residues 198–491, when expressed in *E. coli*, was phosphorylated at Ser378 and Ser382 (Xu et al., 2002). This study showed that mutation of Ser382 to Ala inactivated the WNK1 enzyme, whereas mutation of Ser378 to Ala only moderately reduced activity (Xu et al., 2002). In our peptide-mapping studies with endogenously expressed full-length WNK1 we have not been able to detect phosphorylation of Ser378.

Our findings suggest that, in mammalian cells, phosphorylation of Ser382 may be mediated by a transautophosphorylation reaction. This conclusion is based on the finding that wild-type WNK1, but not kinase-inactive WNK1, when expressed in *E. coli*, is phosphorylated at Ser382 (Fig. 3, B and C). In contrast, we observe that a catalytically inactive WNK1 mutant is normally phosphorylated at Ser382 in response to sorbitol when expressed in 293 cells (Fig. 3). These observations could be explained by the ability of endogenous WNK1 to transphosphorylate the kinase-inactive WNK1 mutant at Ser382 (Fig. 3). However, our data do not rule out the possibility that there is another upstream kinase capable of phosphorylating Ser382 in response to hyperosmotic stress. Nor do our data rule out the possibility that hyperosmotic stress stimulates phosphorylation of Ser382 by inhibiting a protein phosphatase.

Further work is required to establish the roles of the novel sites of phosphorylation on WNK1 that we have identified. Apart from Ser382 (Fig. 3), we have also analyzed the effects that mutating other sorbitol-stimulated phosphorylation sites (Ser167, Ser1261, Thr1848, and Ser2372) had on regulating the activity of WNK1 expressed in 293 cells. We observed that individual mutation of these residues to either Ala or Glu did not markedly affect basal or sorbitol-stimulated WNK1 activity (unpublished data). We suggest that phosphorylation of Ser1261 inhibits the interaction with the CCT domain of SPAK and OSR1 (Fig. 4). There are four RFXV/I motifs in the C-terminal region of WNK1, and a Ser or Thr residue follows all of these potential CCT binding sites. Interestingly, a Ser/Thr residue also follows several other RFXV/I motifs in other proposed SPAK/OSR1 binding proteins, including WNK4, NKCC2, and NCC. It is possible that phosphorylation of residues following RFXV/I motifs comprises a mechanism for dissociating WNK1 from the CCT domains of SPAK and OSR1. We have attempted to detect dissociation of SPAK/OSR1 from WNK1 after sorbitol stimulation of cells but have not observed a marked decrease in the association between SPAK/OSR1 and WNK1. It is possible that nonstoichiometric phosphorylation of Ser1261 and/or the presence of other RFQV/I SPAK/OSR1 binding sites in WNK1 masks detection of the dissociation of SPAK/OSR1 from WNK1 in such an experiment.

We establish that hyperosmotic stress induces activation and phosphorylation of endogenous SPAK and OSR1 at their T-loop and S-motif, the sites phosphorylated by WNK1 in vitro (Fig. 5). Moreover, depletion of WNK1 by ~90% using siRNA methodology markedly inhibited T-loop and S-motif phosphorylation of SPAK/OSR1 and repressed basal and sorbitol-induced activation of these enzymes. Other isoforms of WNK or the remaining low level of WNK1 in these cells may mediate the residual SPAK/OSR1 phosphorylation and activity.

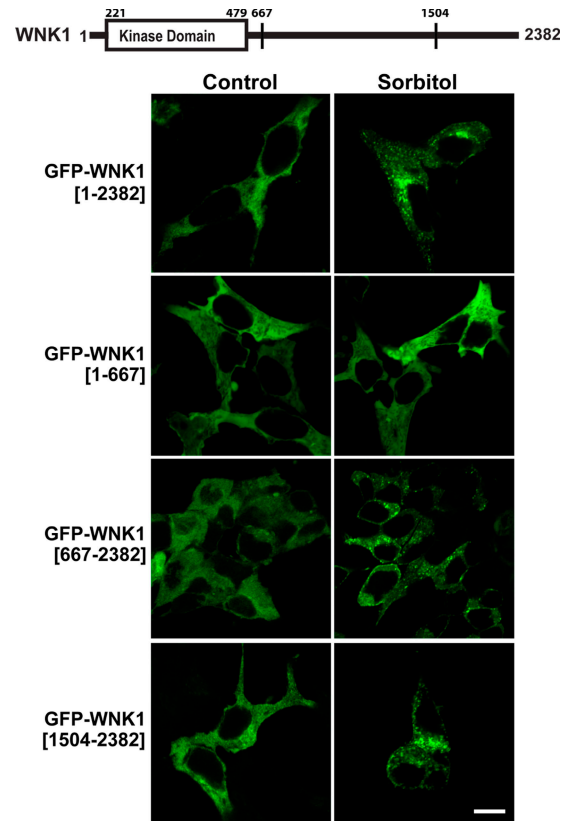


Figure 9. **The C-terminal noncatalytic region of WNK1 mediates translocation to intracellular vesicles.** 293 cells were transfected with the indicated constructs encoding GFP-tagged WNK1. 24 h after transfection, the cells were left untreated or treated with 0.2 M sorbitol for 5 min and analyzed for cell fluorescent imaging using a confocal microscope. Similar results were obtained in two independent experiments. Bar, 10  $\mu$ m.

These data provide further evidence that SPAK/OSR1 are indeed regulated by WNK1 in vivo. While this study was under review, it was reported that siRNA knock down of WNK1 reduced OSR1 activity as well as its total phosphorylation in sorbitol-treated cells, but the sites of phosphorylation affected by WNK1 knockdown were not investigated in this study (Anselmo et al., 2006). Our mutational analysis also confirms that phosphorylation of the T-loop of SPAK/OSR1 is required for sorbitol-induced activation of these enzymes (Fig. 5, B and C). Moreover, we find that individual mutation of the T-loop or S-motif does not affect phosphorylation of the other residue in sorbitol-stimulated cells.

We observed that hyperosmotic stress (sorbitol and NaCl) induced a striking relocalization of WNK1 to intracellular vesicles that are highly mobile (Videos 1 and 2) and colocalize with clathrin, AP-1, and partially with TGN46, but not with the endosomal markers EEA1, Hrs, LAMP1, or AP-2, which colocalizes with plasma membrane-coated pits (Figs. 6 and 7). These results are consistent with the notion that after hyperosmotic stress, a considerable pool of WNK1 is localized to TGN/recycling endosomes. We have not been able to demonstrate that endogenous clathrin and WNK1 coimmunoprecipitate with each other from sorbitol-stimulated cells (unpublished data), indicating that these proteins may not interact directly. The trafficking

of several ion channels and cotransporters between intracellular vesicles and plasma membrane (see Introduction) is strongly influenced by the overexpression of WNK isoforms. It is therefore possible that relocalization of WNK1 to TGN/recycling endosomes may enable it to regulate trafficking and/or activity of certain ion channels/cotransporters. Our findings based on the overexpression of fragments of WNK1 in 293 cells indicate that a C-terminal noncatalytic region of WNK1 mediates this relocalization (Fig. 9). Overexpression of catalytically inactive WNK1 or -4 decreased the membrane expression of the renal outer medullary potassium channel (ROMK) through a clathrin-dependent endocytosis mechanism (Kahle et al., 2003; Cope et al., 2005). Overexpression of the C-terminal noncatalytic region of WNK3 decreased membrane expression of the potassium channel (Leng et al., 2006), and the C-terminal portion of WNK4 coimmunoprecipitated with ROMK in 293 cells (Kahle et al., 2003). Overall, these data suggest that the C-terminal portion of the WNK isoforms plays an important role in influencing WNK cellular localization and function.

In conclusion, our study defines the striking effects that exposure of cells to hyperosmotic conditions has on WNK1 phosphorylation, cellular localization, and catalytic activity as well as on its ability to interact with and activate its substrates SPAK and OSR1. In future studies, it would be important to determine whether the capacity of hyperosmotic stress to stimulate WNK1 and SPAK/OSR1 plays a role in controlling cell volume and blood pressure. It will also be interesting to establish whether the reported effects that WNK isoforms have on ion channels and other cotransporters are mediated through activation of SPAK/OSR1 and/or translocation of WNK1 to TGN/recycling endosomes. It would also be essential to address whether WNK2, -3, and -4 isoforms are regulated in a manner similar to WNK1.

## Materials and methods

### Antibodies

The following antibodies were raised in sheep and affinity purified on the appropriate antigen: the SPAK/OSR1 (total) antibody was raised against the human full-length SPAK and OSR1 proteins, and the SPAK/OSR1 (T-loop) phospho-T233/T185 antibody was raised against a phosphopeptide encompassing residues 226–238 of human SPAK or residues 178–190 of human OSR1 (TRNKVRKTPFVGTGTP). The SPAK/OSR1 (S-motif) phospho-S373/S325 was raised against a phosphopeptide encompassing residues 367–379 of human SPAK (RRVPGSSpGHLHKT), which is highly similar to residues 319–331 of human OSR1 in which the sequence is RRVPGSSpGRLHKT. The antibody used for immunoblotting WNK1, termed WNK1 (total), was raised in sheep against a fragment encompassing residues 61–661 of human WNK1. The antibody used for immunoprecipitation of WNK1, termed WNK1(CT), was raised against a peptide encompassing residues 2360–2382 of human WNK1 (QNFNISNLQKSISNPPGSNLRIT).

The PKB (total) antibody was raised in sheep against a peptide encompassing residues 466–480 of rat PKB $\alpha$  (RPMFPQFSYSASGTA). The following antibodies were purchased from Cell Signaling: ERK1/2 (total), ERK1/2 phospho-Thr202/Tyr204, p38 $\alpha$  (total), p38 $\alpha$  phospho-Thr180/Tyr182, and PKB phospho-Thr308. The JNK (total) and JNK phospho-Thr183/Tyr185 antibodies were obtained from Biosource International. The mouse monoclonal antibody recognizing the GST tag was purchased from Roche. Secondary antibodies coupled to horseradish peroxidase used for immunoblotting were obtained from Pierce Chemical Co. For Li-COR analysis, the IRDye 800-conjugated anti-sheep antibody was purchased from Rockland. Preimmune IgG used in control immunoprecipitation experiments were affinity purified from preimmune serum using protein G-Sepharose. The clathrin antibody was purchased from Abcam, the EEA1

and LAMP1 antibodies (raised in mouse) were purchased from BD Biosciences, and the Hrs antibody was a gift from H. Stenmark (The Norwegian Radium Hospital, Oslo, Norway) and has been described previously (Raiborg et al., 2001). The AP-1 antibody (monoclonal anti- $\gamma$ -adaptin AP6) was obtained from Sigma-Aldrich. The AP-2 antibody (monoclonal anti- $\alpha$ -adaptin) was obtained from Affinity BioReagents, Inc. The TGN46 antibody (polyclonal produced in sheep) was purchased from Serotec. Alexa Fluor 488 donkey anti-sheep, Alexa Fluor 595 donkey anti-rabbit, and Alexa Fluor 595 donkey anti-mouse secondary antibodies were obtained from Invitrogen.

### Immunoprecipitation and assay of WNK1

Anti-WNK1(CT) and preimmune IgG antibodies were covalently coupled to protein G-Sepharose (1  $\mu$ g of antibody per 1  $\mu$ l of beads) using a dimethyl pimelimidate cross-linking procedure. 0.5 mg of clarified cell lysate was incubated with 5  $\mu$ g of anti-WNK1(CT) or preimmune IgG antibody conjugated to 5  $\mu$ l of protein G-Sepharose and incubated for 1 h at 4°C with gentle agitation. The immunoprecipitates were washed twice with 1 ml of lysis buffer containing 0.5 M NaCl and twice with 1 ml of buffer A. The *in vitro* phosphorylation reaction mix contained a final volume of 25  $\mu$ l in buffer A containing 5  $\mu$ M OSR1 [D164A], 0.1 mM [ $\gamma$ -<sup>32</sup>P]ATP, and 10 mM magnesium acetate. The assays were performed for 20 min at 30°C, and the reactions were terminated by adding SDS sample buffer. The samples were electrophoresed on a polyacrylamide gel, which was stained with Coomassie blue, dried, and autoradiographed. The OSR1 Coomassie bands were excised, and incorporation of <sup>32</sup>P-radioactivity was quantified by Cerenkov counting. 1 U of activity was defined as the amount of WNK1 that incorporated 1 nmol of <sup>32</sup>P into OSR1 [D164A]. For experiments in Fig. 3 A using overexpressed forms of GST-WNK1, WNK1 was affinity purified from 0.1 mg of cell lysate using 5  $\mu$ l of glutathione-Sepharose. The beads were washed, and assays were undertaken as described above.

### Immunoprecipitation and assay of SPAK and OSR1

3 mg of clarified cell lysate was incubated with 5  $\mu$ g of the SPAK/OSR1 (total) antibody conjugated to 5  $\mu$ l of protein G-Sepharose and incubated for 1 h at 4°C with gentle agitation. The immunoprecipitates were washed twice with 1 ml of lysis buffer containing 0.5 M NaCl and twice with 1 ml of buffer A. The SPAK/OSR1 immunoprecipitates were either assayed with the CATCHtide peptide substrate (RRHYDDTHTNTYYLRFTGHNTRR) that encompasses the SPAK/OSR1 phosphorylation sites on NKCC1 (Vitari et al., 2006) or using the N-terminal fragment of NKCC1 encompassing residues 1–260 (NKCC1[1–260]; Vitari et al., 2005). Assays were set up in a total volume of either 50  $\mu$ l (CATCHtide assay) or 25  $\mu$ l (NKCC1 assay) in buffer A containing 10 mM MgCl<sub>2</sub>, 0.1 mM [ $\gamma$ -<sup>32</sup>P]ATP (~300 cpm/pmol) and 300  $\mu$ M CATCHtide (RRHYDDTHTNTYYLRFTGHNTRR), or 5  $\mu$ M NKCC1[1–260]. After incubation for 10–60 min at 30°C, the reaction mixture was applied onto P81 phosphocellulose paper (for the CATCHtide assay), the papers were washed in phosphoric acid, and incorporation of <sup>32</sup>P-radioactivity in CATCHtide was quantified. For the NKCC1 assay, the reaction was stopped by the addition of SDS sample buffer. The samples were electrophoresed on a polyacrylamide gel, which was stained with Coomassie blue, dried, and autoradiographed. The NKCC1[1–260] Coomassie bands were excised, and incorporation of <sup>32</sup>P-radioactivity was quantified by Cerenkov counting. For experiments in Fig. 5 (B and C) using overexpressed forms of GST-OSR1 and -SPAK, the GST fusion proteins were affinity purified from 0.5 mg of cell lysate using 5  $\mu$ l of glutathione-Sepharose. The beads were washed, and assays were undertaken as described above, using NKCC1[1–260] as a substrate.

### Microscopy and image analysis

293 cells stably expressing GFP-WNK1 at levels similar to that of endogenous WNK1 were described previously (Vitari et al., 2004). In experiments in which the cells were fixed before analysis, the cells were grown on coverslips (no. 1 1/2) and, after stimulation, were fixed for 5 min in freshly prepared 3% vol/vol formaldehyde in PBS. The cells were washed twice in PBS (5 min each wash) and once in PBS containing 0.2% wt/vol Triton X-100, incubated 10 min in PBS-TG (PBS containing 0.2% wt/vol Tween +3% wt/vol of fish skin gelatine), and incubated for 1 h with anti-clathrin/Hrs/AP-2/TGN46 antibodies (diluted 1:1,000 in PBS-TG), anti-EEA1 antibody (diluted 1:100 in PBS-TG), anti-LAMP1 antibody (diluted 1:50 in PBS-TG), or anti-AP-1 (diluted 1:2,500 in PBS-TG). Cells were washed three times in PBS-T (PBS containing 0.2% wt/vol Tween), incubated for 30 min with the secondary antibody diluted 1:500 in PBS-TG, washed three times in PBS-T and once in water, and mounted onto slides using hydromount (National Diagnostics). Images were collected using the

$\alpha$  Plan 100 $\times$  1.45 NA Plan-Fluor objective on a confocal microscope (LSM 510 META; Carl Zeiss Microimaging, Inc.). Fixed cells were imaged at room temperature ( $\sim$ 20°C) and live cells at 37°C. Images were acquired using LSM 510 acquisition software (Carl Zeiss Microimaging, Inc.), and no further processing of images was performed apart from assembling montages in Photoshop/Illustrator (Adobe). Videos were edited in QuickTime Pro. For imaging of endogenous WNK1, untransfected 293 cells were treated as described above except that 5  $\mu$ g/ml of anti-WNK1 (Total) antibody was used. For live-cell imaging, 293 cells stably expressing GFP-WNK1 were grown on 35-mm-diameter glass-bottomed dishes (Willco). Cells were maintained at 37°C and 5% CO<sub>2</sub> by the use of a microscopy incubator chamber (Carl Zeiss Microimaging, Inc.). For each cell, optical sections of 0.5  $\mu$ m were recorded at 2-s (for Videos 1 and 2 and Figs. S2 and S3) or 10-s (Fig. 8) intervals. FRAP was performed using a bleached region of interest defined by the LSM 510 META software. Recovery of fluorescence was monitored by collecting images every second until recovery was complete. See the supplemental text (available at <http://www.jcb.org/cgi/content/full/jcb.200605093/DC1>) for further methodological details.

### Online supplemental material

The supplemental text contains additional methodological details on materials, buffers, and DNA constructs used, as well as protocols used for *in vivo* <sup>32</sup>P-labeling, identification of phosphorylation sites by mass spectrometry, immunoprecipitation, immunoblotting, and siRNA knockdown protocol. Fig. S1 shows that hyperosmotic stress leads to activation and phosphorylation of SPAK and OSR1 in 293 cells. Figs. S2 and S3 show selected time frames of videos of cells treated with sorbitol (Fig. S2 and Video 1) or NaCl (Fig. S3 and Video 2) to illustrate movement of vesicles to which GFP-WNK1 is recruited. Online supplemental material is available at <http://www.jcb.org/cgi/content/full/jcb.200605093/DC1>.

We thank Harold Stenmark for providing the Hrs antibody, Natalia Shpiro and Rodolfo Marquez for synthesis of PD184352 and BIRB0796, Colin Bell and Agnieszka Kieloch for tissue culture, the Sequencing Service (School of Life Sciences, University of Dundee, Scotland) for DNA sequencing, and the Post Genomics and Molecular Interactions Centre for Mass Spectrometry Facilities (School of Life Sciences, University of Dundee, Scotland) and the protein production and antibody purification teams (Division of Signal Transduction Therapy, University of Dundee), coordinated by Hilary McLauchlan and James Hastie, for generation and purification of antibodies.

E. Pozo-Guisado was supported by a Spanish Ministry of Education and Science fellowship. A. Zagorska and F.H. Rafiqi are the recipients of a 4-yr Wellcome Trust Studentship. A.C. Vitari was supported by a Pfizer-sponsored studentship. We thank the Association for International Cancer Research, Diabetes UK, the Medical Research Council, the Moffat Charitable Trust, and the pharmaceutical companies supporting the Division of Signal Transduction Therapy Unit (AstraZeneca, Boehringer-Ingelheim, GlaxoSmithKline, Merck & Co., Inc., Merck KgaA, and Pfizer) for financial support.

Submitted: 16 May 2006

Accepted: 1 December 2006

## References

Anselmo, A.N., S. Earnest, W. Chen, Y.C. Juang, S.C. Kim, Y. Zhao, and M.H. Cobb. 2006. WNK1 and OSR1 regulate the Na<sup>+</sup>, K<sup>+</sup>, 2Cl<sup>-</sup> cotransporter in HeLa cells. *Proc. Natl. Acad. Sci. USA*. 103:10883–10888.

Chen, W., M. Yazicioglu, and M.H. Cobb. 2004. Characterization of OSR1, a member of the mammalian Ste20p/germinal center kinase subfamily. *J. Biol. Chem.* 279:11129–11136.

Cope, G., A. Golbang, and K.M. O'Shaughnessy. 2005. WNK kinases and the control of blood pressure. *Pharmacol. Ther.* 106:221–231.

Darman, R.B., and B. Forbush. 2002. A regulatory locus of phosphorylation in the N terminus of the Na-K-Cl cotransporter, NKCC1. *J. Biol. Chem.* 277:37542–37550.

Delaloy, C., J. Hadchouel, and X. Jeunemaitre. 2005. With-no-lysine kinases: the discovery of a new pathway in hypertension using human genetic studies. *Hypertension*. 46:263–264.

Dowd, B.F., and B. Forbush. 2003. PASK (proline-alanine-rich STE20-related kinase), a regulatory kinase of the Na-K-Cl cotransporter (NKCC1). *J. Biol. Chem.* 278:27347–27353.

Gagnon, K.B., R. England, and E. Delpire. 2006. Volume sensitivity of cation-Cl<sup>-</sup> cotransporters is modulated by the interaction of two kinases:

Ste20-related proline-alanine-rich kinase and WNK4. *Am. J. Physiol. Cell Physiol.* 290:C134–C142.

Gamba, G. 2006. TRPV4: a new target for the hypertension-related kinases WNK1 and WNK4. *Am. J. Physiol. Renal Physiol.* 290:F1303–F1304.

Hirst, J., and M.S. Robinson. 1998. Clathrin and adaptors. *Biochim. Biophys. Acta*. 1404:173–193.

Kahle, K.T., F.H. Wilson, Q. Leng, M.D. Lalioti, A.D. O'Connell, K. Dong, A.K. Rapson, G.G. MacGregor, G. Giebisch, S.C. Hebert, and R.P. Lifton. 2003. WNK4 regulates the balance between renal NaCl reabsorption and K<sup>+</sup> secretion. *Nat. Genet.* 35:372–376.

Kahle, K.T., F.H. Wilson, and R.P. Lifton. 2005. Regulation of diverse ion transport pathways by WNK4 kinase: a novel molecular switch. *Trends Endocrinol. Metab.* 16:98–103.

Kuma, Y., G. Sabio, J. Bain, N. Shpiro, R. Marquez, and A. Cuenda. 2005. BIRB796 inhibits all p38 MAPK isoforms *in vitro* and *in vivo*. *J. Biol. Chem.* 280:19472–19479.

Kurihara, K., M.L. Moore-Hoon, M. Saitoh, and R.J. Turner. 1999. Characterization of a phosphorylation event resulting in upregulation of the salivary Na<sup>+</sup>-K<sup>+</sup>-2Cl<sup>-</sup> cotransporter. *Am. J. Physiol.* 277:C1184–C1193.

Lalioti, M.D., J. Zhang, H.M. Volkman, K.T. Kahle, K.E. Hoffmann, H.R. Toka, C. Nelson-Williams, D.H. Ellison, R. Flavell, C.J. Booth, et al. 2006. Wnk4 controls blood pressure and potassium homeostasis via regulation of mass and activity of the distal convoluted tubule. *Nat. Genet.* 38:1124–1132.

Lenertz, L.Y., B.H. Lee, X. Min, B.E. Xu, K. Wedin, S. Earnest, E.J. Goldsmith, and M.H. Cobb. 2005. Properties of WNK1 and implications for other family members. *J. Biol. Chem.* 280:26653–26658.

Leng, Q., K.T. Kahle, J. Rinehart, G.G. MacGregor, F.H. Wilson, C.M. Canessa, R.P. Lifton, and S.C. Hebert. 2006. WNK3, a kinase related to genes mutated in hereditary hypertension with hyperkalaemia, regulates the K<sup>+</sup> channel ROMK1 (Kir1.1). *J. Physiol.* 571:275–286.

Lytle, C., and B. Forbush III. 1992. The Na-K-Cl cotransport protein of shark rectal gland. II. Regulation by direct phosphorylation. *J. Biol. Chem.* 267:25438–25443.

Min, X., B.H. Lee, M.H. Cobb, and E.J. Goldsmith. 2004. Crystal structure of the kinase domain of WNK1, a kinase that causes a hereditary form of hypertension. *Structure*. 12:1303–1311.

Moriguchi, T., S. Urushiyama, N. Hisamoto, S. Iemura, S. Uchida, T. Natsume, K. Matsumoto, and H. Shibuya. 2005. WNK1 regulates phosphorylation of cation-chloride-coupled cotransporters via the STE20-related kinases, SPAK and OSR1. *J. Biol. Chem.* 280:42685–42693.

Mu, F.T., J.M. Callaghan, O. Steele-Mortimer, H. Stenmark, R.G. Parton, P.L. Campbell, J. McCluskey, J.P. Yeo, E.P. Tock, and B.H. Toh. 1995. EEA1, an early endosome-associated protein. EEA1 is a conserved alpha-helical peripheral membrane protein flanked by cysteine "fingers" and contains a calmodulin-binding IQ motif. *J. Biol. Chem.* 270:13503–13511.

Pacheco-Alvarez, D., P.S. Cristobal, P. Meade, E. Moreno, N. Vazquez, E. Munoz, A. Diaz, M.E. Juarez, I. Gimenez, and G. Gamba. 2006. The Na<sup>+</sup>:Cl<sup>-</sup> cotransporter is activated and phosphorylated at the amino-terminal domain upon intracellular chloride depletion. *J. Biol. Chem.* 281:28755–28763.

Piechotta, K., J. Lu, and E. Delpire. 2002. Cation chloride cotransporters interact with the stress-related kinases Ste20-related proline-alanine-rich kinase (SPAK) and oxidative stress response 1 (OSR1). *J. Biol. Chem.* 277:50812–50819.

Piechotta, K., N. Garbarini, R. England, and E. Delpire. 2003. Characterization of the interaction of the stress kinase SPAK with the Na<sup>+</sup>-K<sup>+</sup>-2Cl<sup>-</sup> cotransporter in the nervous system: evidence for a scaffolding role of the kinase. *J. Biol. Chem.* 278:52848–52856.

Raiborg, C., K.G. Bache, A. Mehlum, E. Stang, and H. Stenmark. 2001. Hrs recruits clathrin to early endosomes. *EMBO J.* 20:5008–5021.

Rohrer, J., A. Schweizer, D. Russell, and S. Kornfeld. 1996. The targeting of Lamp1 to lysosomes is dependent on the spacing of its cytoplasmic tail tyrosine sorting motif relative to the membrane. *J. Cell Biol.* 132:565–576.

Verissimo, F., and P. Jordan. 2001. WNK kinases, a novel protein kinase subfamily in multi-cellular organisms. *Oncogene*. 20:5562–5569.

Vitari, A.C., M. Deak, B.J. Collins, N. Morrice, A.R. Prescott, A. Phelan, S. Humphreys, and D.R. Alessi. 2004. WNK1, the kinase mutated in an inherited high-blood-pressure syndrome, is a novel PKB (protein kinase B)/Akt substrate. *Biochem. J.* 378:257–268.

Vitari, A.C., M. Deak, N.A. Morrice, and D.R. Alessi. 2005. The WNK1 and WNK4 protein kinases that are mutated in Gordon's hypertension syndrome phosphorylate and activate SPAK and OSR1 protein kinases. *Biochem. J.* 391:17–24.

Vitari, A.C., J. Thastrup, F.H. Rafiqi, M. Deak, N.A. Morrice, H.K. Karlsson, and D.R. Alessi. 2006. Functional interactions of the SPAK/OSR1 kinases with their upstream activator WNK1 and downstream substrate NKCC1. *Biochem. J.* 397:223–231.



- Wilson, F.H., S. Disse-Nicodeme, K.A. Choate, K. Ishikawa, C. Nelson-Williams, I. Desitter, M. Gunel, D.V. Milford, G.W. Lipkin, J.M. Achard, et al. 2001. Human hypertension caused by mutations in WNK kinases. *Science*. 293:1107–1112.
- Xu, B., J.M. English, J.L. Wilsbacher, S. Stippec, E.J. Goldsmith, and M.H. Cobb. 2000. WNK1, a novel mammalian serine/threonine protein kinase lacking the catalytic lysine in subdomain II. *J. Biol. Chem.* 275:16795–16801.
- Xu, B.E., X. Min, S. Stippec, B.H. Lee, E.J. Goldsmith, and M.H. Cobb. 2002. Regulation of WNK1 by an autoinhibitory domain and autophosphorylation. *J. Biol. Chem.* 277:48456–48462.
- Xu, B.E., B.H. Lee, X. Min, L. Lenertz, C.J. Heise, S. Stippec, E.J. Goldsmith, and M.H. Cobb. 2005. WNK1: analysis of protein kinase structure, downstream targets, and potential roles in hypertension. *Cell Res.* 15:6–10.
- Zambrowicz, B.P., A. Abuin, R. Ramirez-Solis, L.J. Richter, J. Piggott, H. BeltrandelRio, E.C. Buxton, J. Edwards, R.A. Finch, C.J. Friddle, et al. 2003. Wnk1 kinase deficiency lowers blood pressure in mice: a gene-trap screen to identify potential targets for therapeutic intervention. *Proc. Natl. Acad. Sci. USA*. 100:14109–14114.